RESEARCH ARTICLE | AUGUST 14 2015

Electron collisions with methyl-substituted ethylenes: Cross section measurements and calculations for 2-methyl–2-butene and 2,3-dimethyl–2-butene

Czesław Szmytkowski; Sylwia Stefanowska; Mateusz Zawadzki; Elżbieta Ptasińska-Denga ; Paweł Możejko

J. Chem. Phys. 143, 064306 (2015)
https://doi.org/10.1063/1.4927703

Electron collisions with methyl-substituted ethylenes: Cross section measurements and calculations for 2-methyl–2-butene and 2,3-dimethyl–2-butene

Czesław Szmytkowski,[a] Sylwia Stefanowska, Mateusz Zawadzki, Elżbieta Ptasińska-Denga, and Paweł Możejko
Department of Atomic, Molecular and Optical Physics, Faculty of Applied Physics and Mathematics, Atomic Physics Group, Gdańsk University of Technology, ul. G. Narutowicza 11/12, 80-233 Gdańsk, Poland

(Received 28 May 2015; accepted 21 July 2015; published online 14 August 2015)

We report electron-scattering cross sections determined for 2-methyl–2-butene [$(H_3C)HC{=}C(CH_3)_2$] and 2,3-dimethyl–2-butene [$(H_3C)_2C{=}C(CH_3)_2$] molecules. Absolute *grand*-total cross sections (TCSs) were measured for incident electron energies in the 0.5–300 eV range, using a linear electron-transmission technique. The experimental TCS energy dependences for the both targets appear to be very similar with respect to the shape. In each TCS curve, three features are discernible: the resonant-like structure located around 2.6–2.7 eV, the broad distinct enhancement peaking near 8.5 eV, and a weak hump in the vicinity of 24 eV. Theoretical integral elastic (ECS) and ionization (ICS) cross sections were computed up to 3 keV by means of the additivity rule (AR) approximation and the binary-encounter-Bethe method, respectively. Their sums, (ECS+ICS), are in a reasonable agreement with the respective measured TCSs. To examine the effect of methylation of hydrogen sides in the ethylene [$H_2C{=}CH_2$] molecule on the TCS, we compared the TCS energy curves for the sequence of methylated ethylenes: propene [$H_2C{=}CH(CH_3)$], 2-methylpropene [$H_2C{=}C(CH_3)_2$], 2-methyl–2-butene [$(H_3C)HC{=}C(CH_3)_2$], and 2,3-dimethyl–2-butene [$(H_3C)_2C{=}C(CH_3)_2$], measured in the same laboratory. Moreover, the isomeric effect is also discussed for the C_5H_{10} and C_6H_{12} compounds. © *2015 AIP Publishing LLC.* [http://dx.doi.org/10.1063/1.4927703]

I. INTRODUCTION

Quantitative data on the elementary processes involving electrons are now provided for a variety of molecular targets (see, e.g., in Refs. 1–3). As the majority of the studies on the electron-assisted phenomena deals with compounds of technological importance and of biological or environmental interest, comprehensive sets of the reliable electron-scattering cross sections, electron transport, and rate coefficients are available for that class of species only. However, for many interesting molecular targets, accurate data are still very fragmentary or are not accessible.

Apart from many efforts to find how quantities describing the electron-induced processes for particular target vary with the energy of projectile, there are also attempts to find relations between electron-molecule scattering data and physico-chemical parameters of selected groups of target molecules. Such investigations could provide some insight into the role of microscopic target properties in the scattering events and would also give ability to predict the electron-scattering quantities for targets for which relevant data are not present yet.

The family of ethylenic derivatives, which are formed when the methyl groups (CH_3) are attached to the C=C double bond replacing the successive hydrogen atoms in the ethylene [$H_2C{=}CH_2$] molecule, constitutes a convenient model for studying the response of the electron scattering dynamics on the methyl substitution. The structural formulas for members of such family, discussed in this paper, are shown in Fig. 1. To date, more extensive study on the electron-scattering from methyl-substituted ethylenes is reported in the literature for the ethylene molecule itself and for its smaller methyl substituents: propene [$H_2C{=}CHCH_3$] and 2-methylpropene [$H_2C{=}C(CH_3)_2$] (for comprehensive references, see Refs. 1 and 3). The experimental studies on the electron-scattering for more complex methyl-ethylenes are exceptionally scarce, while theoretical works concerning the electron stimulated processes are not available in the literature as yet. Particularly, for 2-methyl–2-butene [$(H_3C)HC{=}C(CH_3)_2$], only the derivative with respect to energy of electron transmitted current was reported within 1–5 eV.[4] In case of the 2,3-dimethyl–2-butene [$(H_3C)_2C{=}C(CH_3)_2$] molecule, one can find in the literature the low-energy (1–10 eV) electron-impact excitation spectrum obtained with the trapped-electron (TE) technique[5] and the electron transmission spectrum (ETS).[4] However, the aforementioned works present the electron-scattering intensities only in relative units.

The main goal of this work is to provide the electron-scattering absolute data for larger methyl-ethylenes. The total cross section (TCS) absolute values for the electron scattering from 2-methyl–2-butene and 2,3-dimethyl–2-butene are measured from 0.5 to 300 eV in the linear electron-transmission experiment. To extend the TCS data beyond the experimental energy range, up to 3 keV, model calculations are carried out. Furthermore, having in hand the electron-scattering TCS data for the C_2H_4 molecule and for

[a]Electronic mail: czsz@mif.pg.gda.pl

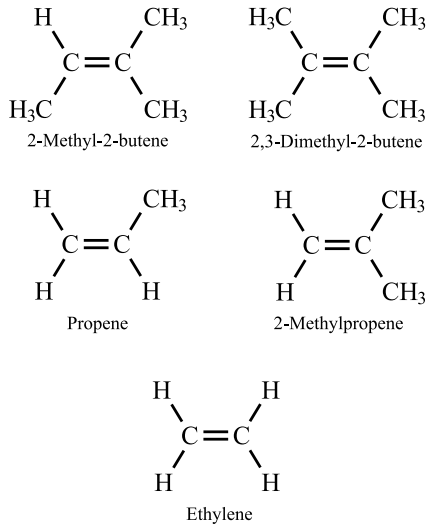

FIG. 1. The condensed structural formulas for the ethylene molecule and its methyl-substituted derivatives.

the family of its methylated derivatives (C_nH_{2n}; n = 3–6), we examine how the replacement of hydrogen atoms with the CH_3 group reflects in the cross section. Finally, to investigate if the arrangement of atoms in the examined target molecules affects the TCS behavior, we compare the present data for 2-methyl–2-butene and 2,3-dimethyl–2-butene with those available for their isomeric counterparts 1-pentene and cyclohexane, respectively.

II. EXPERIMENT

To measure the absolute electron-scattering TCS, we have employed the electron-transmission method in a linear configuration. The electron spectrometer setup and measurement procedures used in this study have been described in detail previously,[6] so only a brief outline on the principle of the experiment is given here. Electron beam of required energy E ($\Delta E \leq 0.1$ eV, FWHM), generated by an electron gun and formed by an electron-optics system consisting of the cylindrical 127° electrostatic monochromator and set of electron lenses, is directed into a reaction chamber filled with a sample vapor. The projectiles, which pass the exit aperture of the chamber, are energetically discriminated with the retarding field lens system and eventually collected by a Faraday cup. The intensity of the magnetic field in the region of the electron trajectory is reduced below 0.1 μT with the system of Helmholtz coils.

In the transmission method, the total scattering cross section, TCS(E), can be derived from the attenuation of a beam of projectiles by target particles using the Bouguer–de Beer–Lambert (BBL) relationship, which adapted to our experiment may be expressed as[6]

$$\mathrm{TCS}(E) = \frac{k\sqrt{T_t T_m}}{p\,L} \ln \frac{I_0(E)}{I_p(E)}, \qquad (1)$$

where $I_p(E)$ and $I_0(E)$ are the intensities of the projectile beam passing a distance L through the reaction volume in the presence and absence of the target molecules, respectively; p refers to the pressure of sample in the scattering cell; T_t stands for the temperature of the target, while T_m = 322 K is the temperature at which the manometer head is maintained; k means the Boltzmann constant.

The effective path length of electrons through the target, L, is given by the linear distance (30.5 mm) between the entrance and exit apertures of the collision cell. The temperature of the target, T_t, was assumed to be equal to that of the scattering chamber, measured with a calibrated semiconductor microsensor. The target pressure, p, in the scattering chamber was measured with the Baratron capacitance manometer head; the pressure readings are corrected for the thermal transpiration effect.[7] Background pressure in the electron optics volume was kept constant at the level of about three orders lower than the target pressure in the scattering cell.[6]

The final absolute TCS value at each impact energy, E, is a weighted mean of results from several series performed at slightly different electron-optics voltage settings and for target pressures ranging from about 30 to 150 mPa; the pressures applied ensure the single-collision conditions in the reaction cell. The TCS uncertainty of a random nature (one standard deviation of the weighted mean TCS value) does not exceed 1% over the whole energy range investigated, except the energies below 1 eV where it increases to 2%.

Accuracy of the measured TCS suffers essentially from numerous possible systematic uncertainties, which may appear while taking the individual quantities necessary for the TCS determination. Some of these uncertainties are characteristic for the electron-transmission technique, as the assumptions at which Eq. (1) is valid are not entirely fulfilled in the real experiment.[8] Unavoidable and the most troublesome systematic uncertainty is associated with the inability to discriminate against electrons, which are scattered elastically through small angles in the forward direction. That *forward scattering effect* not only underestimates the magnitude of the measured TCS but it also might somewhat distort the shape of the TCS energy dependence.[9] As it was not possible to quantify precisely the above-mentioned systematical uncertainty over the whole energy range applied, the final TCS results are not corrected for that effect. Another inevitable error comes from the effusion of target molecules through orifices of the scattering cell leading to inhomogeneity of target density in the reaction volume and to elongation of the effective path over which the scattering events take place.[10] We also noticed that the increasing contamination of the electron optics elements with the target molecules causes a gradual drift in the energy scale during the experiment. The energy drift, by about 0.1 eV, is especially troublesome at low electron-impact energies where the TCS may change steeply with the energy and/or has resonant-like structures. In consequence, the TCS features might be a bit flattened and distorted. Besides, the deposition of target molecules on the electron optics perpetually lowered the intensity of the primary electron current.

The overall systematic uncertainty of our measured absolute TCS amounts up to 9%–12% below 2 eV, 4%–6% within 4–150 eV, and 7%–9% at higher energies applied. The samples (99.5+%), 2-methyl–2-butene and 2,3-dimethyl–2-butene, were purchased from Sigma-Aldrich and distilled by freeze-pump-thaw cycles before use.

III. THEORY AND NUMERICAL CALCULATIONS

To provide the TCS values beyond the energies applied in the present experiment, as well as to analyze the contribution of the elastic and ionization channels to the scattering process, we performed calculations of cross sections for the elastic scattering (ECS) and for the ionization (ICS) induced by the electron collisions with the 2-methyl–2-butene, 2,3-dimethyl–2-butene, and cyclohexane molecules. Employed in this work, theoretical methods and computational procedures are the same as those used in our earlier works;[11,12] thus, only a brief description is provided here.

Elastic cross sections were calculated on the static-polarization level applying the additivity rule (AR) approximation,[13] in which the problem of the electron-molecule scattering is reduced to the electron scattering by atoms constituting the molecular target. In consequence, cross sections derived in this approach are reasonable for intermediate- and high-collision energies only.[11,14]

The integral elastic electron-molecule scattering cross section (ECS) within AR method is given by

$$\sigma_{el}(E) = \frac{4\pi}{k}\sum_{i=1}^{N}\mathrm{Im}f_i(\theta=0,k) = \sum_{i=1}^{N}\sigma_i^A(E), \qquad (2)$$

where E is an energy of the incident electron, $f_i(\theta,k)$ is the scattering amplitude due to the ith atom of the molecule, θ is the scattering angle, and $k=\sqrt{2E}$ means the wave number of the incident electron. The atomic elastic cross section for the ith atom of the target molecule, $\sigma_i^A(E)$, is computed according to

$$\sigma^A = \frac{4\pi}{k^2}\left(\sum_{l=0}^{l_{max}}(2l+1)\sin^2\delta_l + \sum_{l=l_{max}+1}^{\infty}(2l+1)\sin^2\delta_l^{(B)}\right). \qquad (3)$$

To obtain phase shifts, δ_l, partial wave analysis is employed and the proper radial Schrödinger equation

$$\left[\frac{\mathrm{d}^2}{\mathrm{d}r^2} - \frac{l(l+1)}{r^2} - 2(V_{\mathrm{stat}}(r)+V_{\mathrm{polar}}(r)) + k^2\right]u_l(r) = 0 \qquad (4)$$

is solved numerically under the boundary conditions

$$u_l(0)=0, \qquad u_l(r)\xrightarrow{r\to\infty} A_l\hat{\jmath}_l(kr) - B_l\hat{n}_l(kr), \qquad (5)$$

where $\hat{\jmath}_l(kr)$ and $\hat{n}_l(kr)$ are the Riccati-Bessel and Riccati-Neumann functions, respectively. The phase shifts, δ_l, are connected with the asymptotic form of the wave function, $u_l(r)$, by the equation

$$\tan\delta_l = \frac{B_l}{A_l}. \qquad (6)$$

The electron-atom interaction is represented by the static, $V_{\mathrm{stat}}(r)$,[15] and polarization, $V_{\mathrm{polar}}(r)$,[16] potentials, which are given by following expressions:

$$V_{\mathrm{stat}}(r) = -\frac{Z}{r}\sum_{m=1}^{3}C_m\exp(-\beta_m r), \qquad (7)$$

where Z stays for the nuclear charge of the atom and C_m and β_m are parameters obtained by numerical fitting to the numerical Dirac-Hartree-Fock-Slater screening function,[15]

$$V_{\mathrm{polar}}(r) = \begin{cases} \nu(r) & r \le r_c \\ -\alpha/2r^4 & r > r_c \end{cases}, \qquad (8)$$

where $\nu(r)$ is the free-electron-gas correlation energy,[17] α is the static electric dipole polarizability of atom, and r_c is the first crossing point of the $\nu(r)$ and $-\alpha/2r^4$ curves.[18]

In the present calculations, the exact phase shifts, δ_l, are calculated up to $l_{max}=50$, while those remaining, $\delta_l^{(B)}$, are included through the Born approximation.

Electron-impact ICSs presented in this work were calculated using the well known binary-encounter-Bethe (BEB) formalism.[19] In this model formalism, the electron-impact ionization cross section per each molecular orbital is simply given by

$$\sigma^{BEB} = \frac{S}{t+u+1}\left[\frac{\ln t}{2}\left(1-\frac{1}{t^2}\right)+1-\frac{1}{t}-\frac{\ln t}{t+1}\right], \qquad (9)$$

where $u=U/B$, $t=T/B$, $S=4\pi a_0^2 N R^2/B^2$ ($a_0=0.5292$ Å, $R=13.61$ eV), and T is the energy of incident electrons. The electron binding energy, B, kinetic energy of the orbital, U, and the orbital occupation number, N, were obtained for the ground state of the geometrically optimized (within a proper symmetry group) target molecule with the Hartree-Fock method using the GAUSSIAN code[20] and the Gaussian 6-31G++ basis set. As the ionization energies obtained this way usually differ slightly from experimental ones, the outer valence Green function calculations of correlated electron affinities and ionization potentials[21–24] were also performed with the GAUSSIAN. The calculated ionization threshold for the 2-methyl–2-butene molecule is equal to 8.580 eV. Whereas for 2,3-dimethyl–2-butene and cyclohexane, it is 8.193 eV and 10.402 eV, respectively.

Finally, the total cross section, σ^{Ion}, for electron-impact ionization of molecule can be obtained as

$$\sigma^{\mathrm{Ion}} = \sum_{i=1}^{n_{\mathrm{MO}}}\sigma_i^{BEB}, \qquad (10)$$

where n_{MO} is the number of the given molecular orbital.

To compare our computational results with the experimental TCSs, we finally summed the calculated ECSs and ICSs at respective energies. While obtaining this way, ECS+ICS is rather an approximation of the total cross section, we found that for intermediate energies, the calculated TCSs agree reasonably with those measured for a wide variety of target molecules (see, e.g., Refs. 25–31).

IV. RESULTS AND DISCUSSION

In this section, we report on absolute *grand*-TCS measurements for electron collision with the 2-methyl–2-butene [$(H_3C)HC{=}C(CH_3)_2$] and 2,3-dimethyl–2-butene [$(H_3C)_2C{=}C(CH_3)_2$] molecules. The measurements were carried out in the linear electron-transmission experiment over an incident energy range from 0.5 to 300 eV. We also present integral ECS and ICS for electron collision with the 2-methyl–2-butene, 2,3-dimethyl–2-butene, and cyclohexane

[c-C_6H_{12}] molecules, calculated in the AR approximation and the BEB approach, respectively, for energies up to 3 keV. The sums, ECS+ICS, are then compared with the measured TCSs at energies of overlap. Furthermore, we confront our earlier experimental TCS for the ethylene molecule with those measured for the family of methyl-substituted ethylenes: propene, 2-methylpropene, 2-methyl–2-butene, and 2,3-dimethyl–2-butene; for their structural formulas, see Fig. 1, while for selected properties, see Table III. Similarities and differences of compared TCS energy functions are pointed out and discussed. Finally, we compare TCSs measured for 2-methyl–2-butene and 2,3-dimethyl–2-butene with experimental TCSs available for their respective isomeric counterparts, 1-pentene[30] and cyclohexane,[32] to examine how the arrangements of atoms in isomers of C_5H_{10} and C_6H_{12} compounds reflect in the electron-scattering cross section.

A. Cross sections for 2-methyl–2-butene [$(H_3C)HC{=}C(CH_3)_2$] and 2,3-dimethyl–2-butene [$(H_3C)_2C{=}C(CH_3)_2$]

Figures 2(a) and 2(b) show our experimental absolute TCS results for electron scattering from the 2-methyl–2-butene (C_5H_{10}) and 2,3-dimethyl–2-butene (C_6H_{12}) molecules as a function of the electron incident energy, in the range from 0.5 to 300 eV. Numerical TCS results for the both molecular targets are listed in Table I. The computed ECS and ICS are also plotted in Figs. 2(a) and 2(b); their values up to 3 keV are presented in Table II. In addition, for the both targets, the sums of ECS and ICS are shown in Figs. 2(a) and 2(b) to compare with the experimental TCS findings. No other absolute electron-scattering results for the considered targets are available in the literature for comparison.

The magnitude of the experimental TCS for the 2-methyl–2-butene molecule (see Table I) is systematically lower than that for 2,3-dimethyl–2-butene, over the whole investigated energy range. A nearly constant ratio of the compared TCSs is mainly associated with a difference in the molecular size of the both considered targets; the 2-methyl–2-butene molecule contains one methyl group less than the 2,3-dimethyl–2-butene (see Fig. 1). According to the shape, the TCS energy curve for 2,3-dimethyl–2-butene closely resembles that for 2-methyl–2-butene—characteristic TCS features for both species are located at nearly the same energies. Between 0.5 and 1.3 eV, the TCSs for both C_5H_{10} and C_6H_{12} compounds are rather slowly varying functions of the energy and their values lie within $20–22 \times 10^{-20}$ m^2 and $24–26 \times 10^{-20}$ m^2, respectively. From 1.4 eV, the considered TCS curves increase rapidly with the energy and reach their first maximum (of 46×10^{-20} m^2 and 48×10^{-20} m^2, respectively) centered at 2.6–2.7 eV. Note that the 2.7 eV structure for C_6H_{12} is less marked than that around 2.6 eV for the C_5H_{10} molecule. The both TCS energy functions have a local minimum near 3 eV and, when the impact energy still increases, they rise again and show a pronounced broad enhancement spanned between 4 and 16 eV, peaking at 8–9 eV with a value of 72×10^{-20} m^2 and 84×10^{-20} m^2, respectively. Above 10 eV, the magnitude of TCSs starts to decrease with the energy increase. However, within 20–26 eV, a weak hump

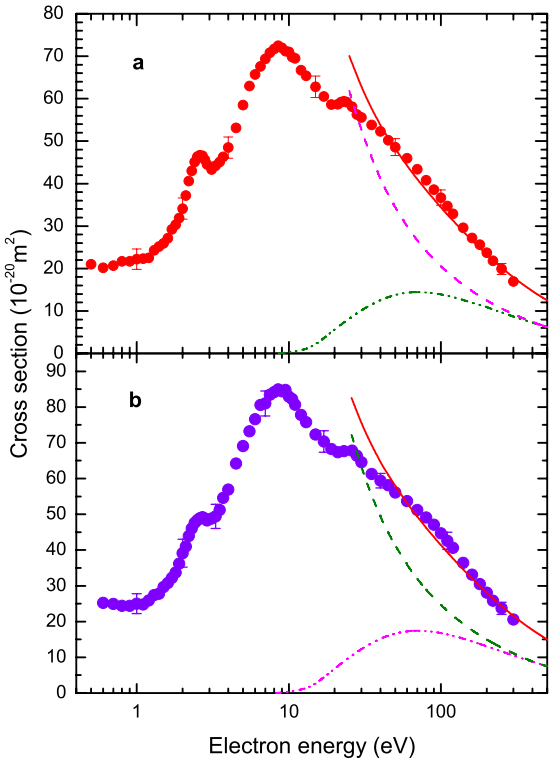

FIG. 2. Cross sections for the electron scattering from the 2-methyl–2-butene and 2,3-dimethyl–2-butene molecules. (a) The 2-methyl–2-butene [$(H_3C)HC{=}C(CH_3)_2$] molecule: experimental absolute TCS (full red circles), present, the error bars denote overall (systematic+statistical) uncertainties; (dashed-doted-doted olive line), the ionization cross section (ICS), computed with the BEB approach; (dashed magenta line), the elastic cross section (ECS), computed using the AR method; the full red line represents the sum ECS+ICS. (b) The 2,3-dimethyl–2-butene [$(H_3C)_2C{=}C(CH_3)_2$] molecule: absolute TCS (full violet circles), present experiment, the error bars denote overall uncertainties; (dashed-doted-doted magenta line), ionization cross section (ICS), computed with the BEB approach; (dashed green line), elastic cross section (ECS), computed using the AR method; the full red line represents the sum ECS+ICS.

in each TCS curve (by $1–2 \times 10^{-20}$ m^2 above the background) is clearly discernible. Beyond 30 eV, the TCS energy functions decline monotonically and around 300 eV fall to about 17×10^{-20} m^2 for 2-methyl–2-butene and 21×10^{-20} m^2 for 2,3-dimethyl–2-butene.

Such a close similarity in the shape of TCS curves for the 2-methyl–2-butene and 2,3-dimethyl–2-butene molecules implies that the low-energy TCS features (located at 2.6–2.7, 4–16, and 20–26 eV) may have the same physical origin for both targets. The scarcity of experiments on the low-energy electron-scattering from the considered targets and absence of theoretical investigations make the interpretation of the observed TCS features, especially these located within 4–16 eV and 20–26 eV, rather difficult and somewhat speculative. Concerning the TCS peaks centered at 2.6–2.7 eV, there are some indications, provided by the electron transmission spectroscopy[4] and the trapped electron excitation spectra[5] that within the 1.5–3.5 eV energy range, the resonant processes contribute to the scattering. The origin of TCS structures observed within 4–16 eV and 20–26 eV can have, at least in part, the resonant character; however, their assignment is less certain.

TABLE I. Absolute total cross sections (TCS) measured for electron impact on the 2-methyl–2-butene (C_5H_{10}) and 2,3-dimethyl–2-butene (C_6H_{12}) molecules, in units of 10^{-20} m^2.

	TCS			TCS			TCS	
Energy (eV)	C_5H_{10}	C_6H_{12}	Energy (eV)	C_5H_{10}	C_6H_{12}	Energy (eV)	C_5H_{10}	C_6H_{12}
0.5	21.0		3.1	43.3	48.8	22	59.2	
0.6	20.2	25.2	3.3	44.2	49.4	23	59.4	67.7
0.7	20.7	24.8	3.5	45.1	51.2	24	59.2	
0.8	21.7	24.4	3.7	46.3	54.6	26	58.1	67.8
0.9	21.7	24.4	4.0	48.5	56.9	28	56.3	66.4
1.0	22.2	25.0	4.5	53.1	64.2	30	55.6	64.6
1.1	22.3	24.8	5.0	58.5	69.1	35	53.8	61.3
1.2	22.5	25.9	5.5	63.0	73.2	40	52.3	59.4
1.3	24.3	27.4	6.0	65.7	76.6	45	50.2	58.1
1.4	25.2	27.8	6.5	67.6	80.6	50	48.6	56.1
1.5	25.9	29.7	7.0	69.4	81.0	60	46.0	53.7
1.6	27.1	30.8	7.5	70.8	83.4	70	43.4	51.2
1.7	29.2	32.2	8.0	71.7	84.2	80	40.8	49.1
1.8	30.3	33.7	8.5	72.5	84.9	90	38.6	47.1
1.9	31.9	36.2	9.0	72.0	84.4	100	36.7	44.7
2.0	34.1	39.1	9.5	71.2	84.8	110	34.7	42.6
2.1	37.2	41.0	10.0	71.0	82.9	120	32.9	40.6
2.2	40.6	43.9	10.5	69.8	82.2	140	29.6	36.4
2.3	43.0	46.0	11	69.5	80.7	160	27.2	33.1
2.4	45.1	47.6	12	66.7	77.8	180	25.6	30.5
2.5	46.4	48.4	13	65.4	75.8	200	23.7	28.1
2.6	46.7	48.9	15	62.8	72.3	220	21.9	25.8
2.7	46.5	49.2	17	60.5	70.4	250	19.9	23.7
2.8	45.6	48.8	19	58.6	68.3	300	16.9	20.6
2.9	44.5	48.3	21	58.7	67.4			

In the aim of the further support of our statement on the resonant origin of the TCS features for 2-methyl–2-butene [$(H_3C)HC{=}C(CH_3)_2$] and 2,3-dimethyl–2-butene [$(H_3C)_2C{=}C(CH_3)_2$], we turn to electron-impact studies for ethylene [$H_2C{=}CH_2$] and its methyl substituted derivatives: propene [$H_2C{=}CH(CH_3)$] and 2-methylpropene [$H_2C{=}C\text{-}(CH_3)_2$]. The afore-mentioned compounds, along with the 2-methyl–2-butene and 2,3-dimethyl–2-butene molecules, form a molecular alkenes family, C_nH_{2n}, in which the successive members differ in the number of methyl (CH_3) groups replacing the hydrogen atoms in the ethylene molecule (see Fig. 1).

Figure 3 depicts the experimental TCSs energy dependences for ethylene and its methylated derivatives: propene, 2-methylpropene, 2-methyl–2-butene, and 2,3-dimethyl–2-butene. To keep conformity, all displayed TCS results are taken from experiments performed in our laboratory.[28,33–35] It is evident from Fig. 3 that the compared TCS curves show a very similar behavior over the whole investigated energy range. The low-energy pattern visible in the TCS curve for ethylene is also perceptible in TCSs for larger members of the examined family. At the same time, as the number of methyl groups in a target molecule increases, some new TCS structures become more visible at higher impact energies. Each TCS energy function in Fig. 3 has the low-energy peak; the position of this peak (see Table III) shows the steady shift in energy (from 1.9 eV for ethylene to 2.7 eV for 2,3-dimethyl–2-butene), while its amplitude becomes less pronounced with the number of methyl groups increased. The shift of the low-energy TCS resonant peak toward higher energies, across the series, and the lowering of its amplitude may be associated with the redistribution of the electric charge in the methyl-substituted molecules due to interaction of methyl group orbitals with the C=C orbitals.[4,36] An interesting observation is that, at energies above 4 eV, the TCS for the every next methylated molecule increases—by nearly the same value—with the number of methyl groups attached around the C=C bond. The TCS for these targets also appears to approximately scale with their electric dipole polarizability (see Table III).

Studies for the ethylene molecule demonstrated clearly the resonant character of the electron scattering within 1–3 eV energy range.[4,5,37–41] A temporary accommodation of an incident electron (of the energy around 1.9 eV) in the molecular π^* orbital of the ethylene electronic ground state, with the formation of the parent negative ion (the shape-resonant state), leads to dominant excitation of the C=C stretch vibrations in the target molecule after the anion eventually decays through the autodetachment of the extra electron.[4,38,40,41] The short-lived negative ion state can decompose also throughout the decay into negative stable fragment and neutrals.[39] This π^* resonance leads to a distinct increase of the vibrational cross sections for the ethylene molecule between 1 and 3 eV and, in consequence, to the peak in the TCS centered at 1.9 eV. The similarity between the 2-methyl–2-butene and 2,3-dimethyl–2-butene molecular conformations, as well as similarity of the 2–3.5 eV features

TABLE II. Ionization (ICS) and integral elastic (ECS) cross sections calculated for electron impact on the 2-methyl–2-butene (C_5H_{10}) and 2,3-dimethyl–2-butene (C_6H_{12}) molecules, in 10^{-20} m^2.

	ICS			ICS		ECS	
Energy (eV)	C_5H_{10}	C_6H_{12}	Energy (eV)	C_5H_{10}	C_6H_{12}	C_5H_{10}	C_6H_{12}
8.193		0	50	13.8	16.7	34.4	41.3
8.580	0		55	14.1	17.1		
9.0	0.0827	0.178	60	14.3	17.3	29.9	35.8
10	0.290	0.408	65	14.4	17.4		
11	0.497	0.649	70	14.4	17.4	26.6	31.9
12	0.763	0.956	75	14.4	17.4		
13	1.089	1.322	80	14.4	17.3	24.1	28.9
14	1.57	1.960	85	14.3	17.2		
15	2.19	2.70	90	14.2	17.1	22.1	26.6
16	2.89	3.55	95	14.0	16.9		
17	3.60	4.43	100	13.9	16.8	20.5	24.6
18	4.30	5.28	110	13.6	16.4	19.2	23.0
19	4.98	6.10	120	13.3	16.0	18.0	21.6
20	5.61	6.86	140	12.6	15.2	16.1	19.3
22.5	7.03	8.56	160	12.0	14.5	14.7	17.6
25	8.23	9.99	180	11.4	13.7	13.5	16.2
27.5	9.27	9.25	200	10.8	13.1	12.5	15.0
30	10.2	12.3	220	10.3	12.4	11.6	14.0
35	11.6	14.0	250	9.64	11.6	10.6	12.7
40	12.6	15.3	300	8.69	10.5	9.23	11.1
45	13.3	16.1	350	7.91	9.55	8.21	9.85
			400	7.27	8.77	7.40	8.88
			450	6.72	8.11	6.74	8.09
			500	6.26	7.55	6.19	7.43
			600	5.51	6.65	5.34	6.40
			700	4.93	5.95	4.69	5.63
			800	4.47	5.39	4.20	5.03
			900	4.09	4.93	3.80	4.56
			1000	3.77	4.55	3.47	4.16
			1500	2.74	3.31	2.49	2.98
			2000	2.17	2.62	1.98	2.37
			2500	1.81	2.18	1.74	2.09
			3000	1.55	1.87	1.66	1.99

TABLE III. Selected electric molecular parameters for considered compounds: the permanent dipole moment, μ, and the static dipole polarizability, α (from Ref. 50, unless specified otherwise). Location of the first maximum, $E_{1\max}$, observed in the TCS curves. The vertical attachment energies, *VAE*, are taken from Ref. 4.

	$E_{1\max}$	*VAE*	μ	α
Molecule	(eV)		(D)	(10^{-30} m^3)
$H_2C{=}CH_2$; ethylene	1.8[a]	1.78	0	4.25
$H_2C{=}CH(CH_3)$; propene	2.2[b]	1.99	0.366	6.26
$H_2C{=}C(CH_3)_2$; 2-methylpropene	2.4[c]	2.19	0.503	8.29
$(H_3C)HC{=}C(CH_3)_2$; 2-methyl–2-butene	2.6[d]	2.24	0.192[e]	9.72[e]
$(H_3C)_2C{=}C(CH_3)_2$; 2,3-dimethyl–2-butene	2.7[d]	2.37	0	12[f]
c-$(CH_2)_3$; cyclopropane			0	5,66
c-$(CH_2)_6$; cyclohexane			0	10.87; 11.0
$H_2C{=}CH(CH_2)_2CH_3$; 1-pentene			0.5	9.65

[a]Reference 33.
[b]Reference 34.
[c]Reference 28.
[d]Present work.
[e]Reference 51.
[f]Estimation based on the additivity formula from Ref. 52.

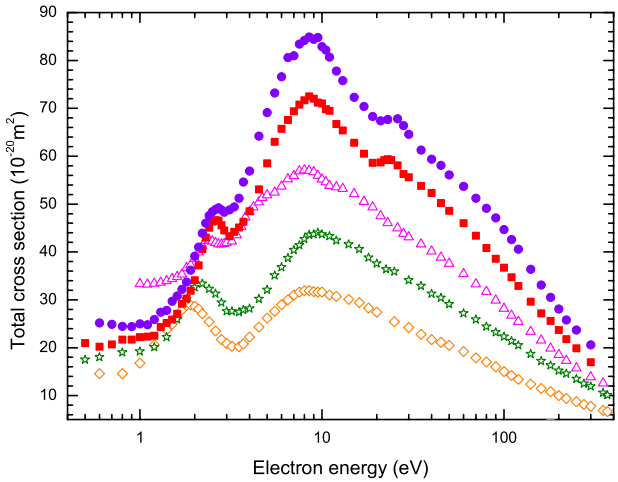

FIG. 3. Experimental total cross sections for electron scattering from the ethylene molecule and its methylated derivatives: 2,3-dimethyl–2-butene [$(H_3C)_2C{=}C(CH_3)_2$], full violet circles, present; 2-methyl–2-butene [$(H_3C)HC{=}C(CH_3)_2$], full red squares, present; 2-methylpropene [$H_2C{=}C(CH_3)_2$], open magenta up-triangles, from Ref. 28; propene [$H_2C{=}CH(CH_3)$], open olive stars, from Ref. 34; and ethylene [$H_2C{=}CH_2$], open orange diamonds, from Ref. 33.

in their TCS curves—to these for ethylene—allows to suppose that the low-energy peak in TCS curves for both methylated species is also associated with the formation of the temporary molecular anion state when the electron of energy around 2.7 eV is captured by these targets in the π^* orbital. More direct support for the resonant origin of the 1.5–3.5 eV feature in the TCS energy functions for the 2-methyl–2-butene and 2,3-dimethyl–2-butene molecules comes from the electron transmission spectroscopy.[4] That experiment also suggested that the methyl substitution may cause a decrease in the lifetime of the negative ion state. For the 2,3-dimethyl–2-butene molecule, a resonant-like structure below 4 eV was also noted in the trapped electron excitation spectra.[5]

Figure 3 shows that the relative amplitude of the broad TCS enhancement spanned between 4 and 15 eV distinctly increases with respect to the first resonant maximum, across a series of considered methyl-substituted ethylenes. Electron-impact investigations on ethylene[37–41] revealed that in this energy regime, further resonant states are created by the trapping of an incident electron in the higher electronic orbitals, which may considerably contribute to the cross section. Above 4.3 eV, the electron-induced excitation of numerous electronic states of 2,3-dimethyl–2-butene was evidenced.[5] Resonant structures for energies between 4 and 12 eV were also observed for propene—the second member of the considered molecular series.[4,37,39,42] It is worth noting that, around 7–10 eV, a similar broad enhancement of the TCS has been already observed for a wide variety of hydrocarbons (alkanes, alkenes, and alkynes) and associated, at least in part, with a creation of the very short-living σ^* resonant states (see, e.g., Ref. 43).

An interesting feature clearly visible in TCS curves for 2-methyl–2-butene and 2,3-dimethyl–2-butene (Fig. 3) is the small hump located around 24 eV. A shoulder in the TCS energy function for 2-methylpropene and a week flattening of TCS curves for ethylene and propene are distinguishable at lower energies, near 15 eV. Similar behavior of the TCS curve has been already observed for series of alkanes[32] and alkynes.[31] Unfortunately, in that energy range, experiments for complex hydrocarbon molecules are less detailed and do not give the exact indication on the character of the scattering dynamics. On the other hand, calculations[44] suggest that beyond 10 eV, numerous weak resonances can contribute to the scattering. More conclusive evidence for the formation of such intermediary resonant states in the electron scattering by molecules requires further experimental and/or theoretical studies of the vibrational and dissociative attachment channels.

Figure 3 also reveals that for energies below 2 eV, the TCS for 2-methylpropene is much higher than for the other methylethylenes. This TCS increase can be related to distinctly higher electric dipole moment (~0.5 D, see in Table III) of the 2-methylpropene molecule, which at low-impact energies substantially increases the contribution from the direct long-range interactions in the scattering event.[45]

In Figs. 2(a) and 2(b), we also compare our TCS measurements with the sum, ECS+ICS, of our calculated integral ECS and ICS for 2-methyl–2-butene and 2,3-dimethyl–2-butene; the ECS+ICS stands for the theoretical TCS estimation. In the range of 50–300 eV, where energies of measurements and calculations overlap, the agreement between the experiment and calculations is good, both with respect to the general shape and magnitude. Within 50 and 250 eV, the divergences do not exceed 6%–8%, falling within typical experimental uncertainty limits. Such an agreement indicates that our calculated high-energy ECS+ICS values can predict reliably the TCS values also at energies far beyond the experimental regime.

In Figs. 2(a) and 2(b) included are also the partial cross sections, ECS and ICS, to illustrate the role of the elastic and ionization processes in the scattering at the intermediate and high energy ranges. The both calculated ECSs are the monotonically decreasing functions of energy over the whole considered range. Note, however, that below 50–80 eV, the obtained ECS becomes more and more overestimated as at low collision energies, the principles of the AR method used for ECS calculations are not physically fulfilled. Above the ionization thresholds, from about 9 eV, the ICS curves for both targets increase with the energy and reach the maximum around 70–75 eV, then they systematically decrease. Comparison shows that at low-intermediate energies, the role of the elastic processes in the scattering is more dominant than the ionization, by about 80% near the ICS maximum, while from near 300 eV, the contribution of both scattering processes becomes comparable.

B. The isomeric effect for C_5H_{10} and C_6H_{12} compounds

In this section, we examine how a different geometrical arrangement of atoms in the isomers of C_5H_{10} and C_6H_{12} compounds manifests itself in the respective electron-impact TCS energy dependences.

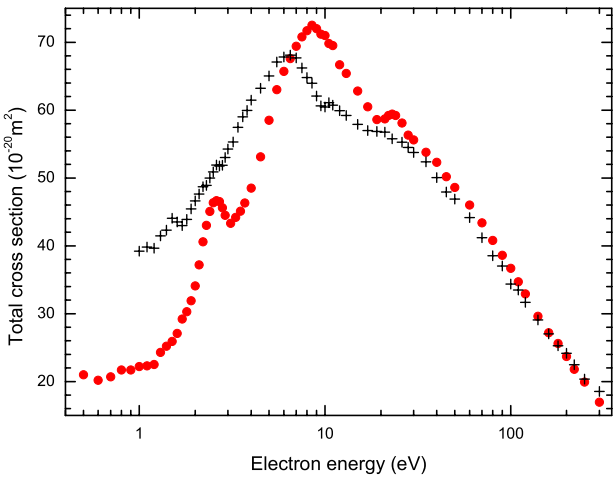

FIG. 4. An illustration of the isomer effect for C_5H_{10} compounds. Compared are the experimental electron-scattering TCS for 2-methyl–2-butene (full red circles), present and 1-pentene (black crosses), from Ref. 30.

1. Isomers of C_5H_{10}: 2-methyl–2-butene $[(H_3C)HC{=}C(CH_3)_2]$ and 1-pentene $[H_2C{=}CH\text{-}(CH_2)_2CH_3]$

Figure 4 compares the present experimental TCS results for 2-methyl–2-butene with TCS data for another C_5H_{10} open-chain isomer, namely, 1-pentene $[H_2C{=}CH\text{-}(CH_2)_2CH_3]$—also measured in our laboratory.[30] In the 2-methyl–2-butene molecule, two CH_3 groups are attached to one end of the C=C bond, while on the opposite side located are one hydrogen atom and one CH_3 group. In the 1-pentene molecule, there are two hydrogen atoms on one side of the C=C bond and one H atom and one propyl group ($CH_2CH_2CH_3$) on the opposite end. This structural difference leads to different electric charge distributions in considered targets. Thus, 1-pentene is a more polar molecule than 2-methyl–2-butene (see Table III). From this comparison, it is clearly seen that a different arrangement of atoms in the considered C_5H_{10} species is reflected mainly in the magnitude of TCS at lower impact energies, below 40 eV. With respect to the general shape, the compared TCS energy dependences are quite similar; although in the low energy range, some differences in the location and distinctness of TCS features are discernible. Near 1 eV, the magnitude of TCS for 1-pentene is nearly twice as high as that for the 2-methyl–2-butene molecule. This difference can be associated with a higher permanent electric dipole moment of the 1-pentene molecule (cf. Table III).[45] The main TCS maximum for 2-methyl–2-butene, located around 8.5 eV, is shifted by 2–3 eV toward higher energies comparing with that for 1-pentene. In this energy regime, the TCS for 2-methyl–2-butene becomes also clearly higher in the magnitude. Similar shift in the energy is visible for the low-energy TCS structure: the distinct peak for 2-methyl–2-butene, at 2.6 eV, for 1-pentene is located around 1.7 eV and is less pronounced. Beyond 40 eV, both examined TCS curves decrease rather monotonously with the energy increase and practically merge, what confirms earlier findings that at intermediate and high impact energies, isomers are not distinguishable respective to TCS.[34,46–48] Such behavior of TCSs for isomers indicates that (i) at low-impact energies, the electron-molecule interaction is determined by the molecular character of the target and the distribution of the electric charge in the molecule as a whole; (ii) starting from intermediate energies, the interaction of the impinging electron with the atomic constituents of target is adequate for the description of the electron-molecule collision and justifies the application of the AR approach for TCS calculations at intermediate and high impact energies.

2. Isomers of C_6H_{12}: $[(H_3C)_2C{=}C(CH_3)_2]$ and cyclohexane $[c\text{-}C_6H_{12}]$

Fig. 5(a) compares the present experimental TCS energy function for the 2,3-dimethyl–2-butene $[(CH_3)_2C{=}C(CH_3)_2]$ molecule to TCS measurements for its isomeric counterpart, cyclohexane $[c\text{-}C_6H_{12}]$, taken from Ref. 32. The 2,3-dimethyl–2-butene is an open chain hydrocarbon, while cyclohexane is a single-ring molecule. According to the general shape, the compared TCS energy functions resemble each other. However, except the energies around 1 eV and near 300 eV, both TCSs differ significantly in the magnitude. Between 2 and 200 eV, the difference amounts even 40% and

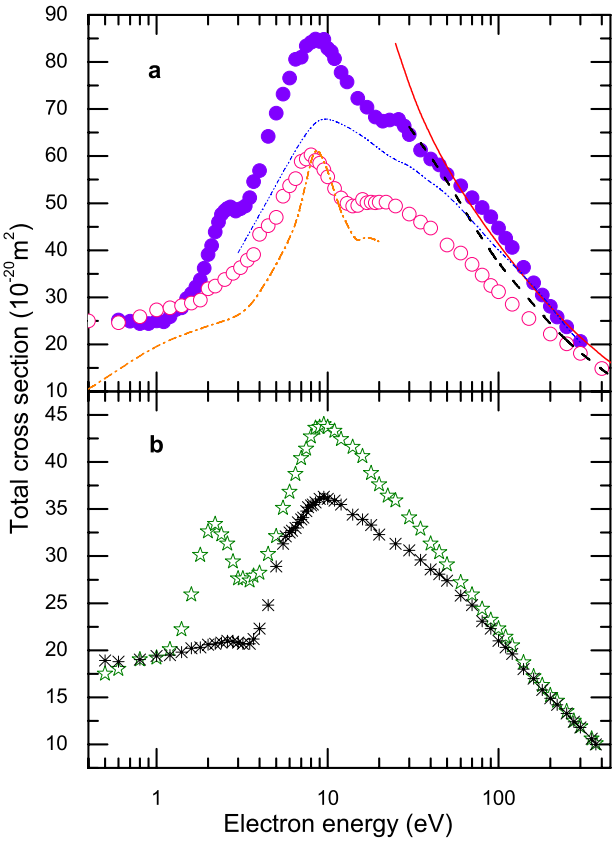

FIG. 5. (a). Experimental electron-scattering TCSs for isomers of the C_6H_{12} compound: 2,3-dimethyl–2-butene (full violet circles), present absolute; cyclohexane (open pink circles), normalized, from Ref. 32. Included are also theoretical cross sections for cyclohexane: (dashed black line), TCS computed using the additivity rule (AR) taking into account the geometrical shielding;[49] (full red line), ECS+ICS, present AR computations; integral elastic cross section (dashed-doted orange line);[53] and estimated (see text) TCS (dashed-doted-doted blue line), present. (b). For comparison presented are experimental TCSs (from Ref. 34) for two isomers of the C_3H_6: propene (open olive stars) and cyclopropane (black asterisks).

is twice higher than the combined declared uncertainties of both experiments.

In the light of TCS results for the isomeric targets obtained hitherto,[34,46–48] such a level of disagreement in the magnitude of TCS curves for isomers of C_6H_{12} compound, especially at energies between 40 and 200 eV, is somewhat intriguing and needs a comment. Typically, TCSs for electron scattering from isomeric molecules do not differ beyond 80–100 eV by more than a few percent (cf. Fig. 4). We suppose that the difference of TCS values for C_6H_{12} isomers at intermediate energies is not related to the difference in the geometrical structures of both targets only; it might rather be associated in part with different experimental conditions, at which TCS values for these two isomers have been obtained. Normalized results for cyclohexane were determined using the transmission time-of-flight (TOF) technique employing the guiding magnetic field (of 0.45 mT) in the scattering volume; to put the TCS on the absolute scale, the path length of electrons through the target was evaluated indirectly.[32] In the present TCS measurements for 2,3-dimethyl–2-butene, the magnetic field was reduced in considerable degree (below 0.1 μT) and all quantities necessary for determination of TCS were obtained directly. Comparisons show (for example, see Ref. 48) that the normalized TCSs obtained with the TOF method (employing the magnetic field) are usually systematically lower by about 10%–20% than absolute TCS results obtained in our laboratory.

For the confirmation that even a drastic change of the structure in the C_6H_{12} isomers cannot be responsible for the observed differences in TCS magnitudes, in Figure 5(b), we show TCS results obtained in our laboratory[34] for two isomers of C_3H_6 compound: propene and cyclopropane. The propene (C_3H_6) molecule is, like 2,3-dimethyl–2-butene (C_6H_{12}), an open-chain compound, while cyclopropane (c-C_3H_6) and cyclohexane (c-C_6H_{12}) are, respectively, their cyclic (single-ring) isomers. While at lower energies, the TCSs for C_3H_6 isomers differ substantially in the magnitude and shape, the differences diminish gradually above 10 eV, and both curves practically merge beyond 80 eV. It is worth noting that the TCSs energy curves for C_3H_6 isomers obtained with the TOF technique are very similar in the shape to these in Fig. 5(b); however, they are again systematically lower in the magnitude (see Ref. 48).

In Fig. 5(a), we also included theoretical TCS values for cyclohexane obtained using two different approximations: one employing the additivity rule taking into account the geometrical shielding[49] and another one using the AR approach described in the present work. Comparison shows that both computed TCSs for cyclohexane lie distinctly above the experimental values from Ref. 32.

Finally, we can roughly estimate the TCS for c-C_6H_{12} based on the observation that above 4 eV, the TCS values for 2,3-dimethyl–2-butene are 1.8–1.9 times higher than those for propene.[34] If we apply the same factor for the cyclic isomers of these compounds, we can obtain the TCS values for cyclohexane based on our data for cyclopropane.[34] Fig. 5(a) shows that estimated this way TCS for cyclohexane is above 10 eV distinctly higher than the experimental data,[32] and beyond 100 eV, it does not differ much from the TCS for 2,3-dimethyl–2-butene. To explain the observed disagreement of the experimental TCSs for C_6H_{12} isomers more definitely, further investigations are required.

V. CONCLUDING REMARKS

In this work, we have measured the absolute electron-scattering TCSs for 2-methyl–2-butene and 2,3-methyl–2-butene molecules from low to intermediate energies, 0.5–300 eV, using the electron transmission method. According to our knowledge, these TCS results are the first reported. The experimental TCS energy dependences for both targets exhibit three distinct features: a resonant-like structure peaked at 2.6–2.7 eV; a pronounced broad enhancement spanned between 4 and 20 eV with the maximum at 8.5 eV, and a weak hump near 24 eV. The observed TCS structures can be explained in terms of the resonant events, superimposed onto the direct scattering processes. For more conclusive assignments, further detailed experimental and theoretical studies are necessary.

Additionally, the integral ECS and ICS have been computed for the both methylated molecular targets and for cyclohexane at intermediate and high electron impact energies. The ECS+ICS values computed for the 2-methyl–2-butene and 2,3-methyl–2-butene molecules agree reasonably well with the experimental TCSs at overlapping energies above 50 eV. For cyclohexane, our intermediate TCS computations are in good agreement with the calculations taking into account the geometrical shielding[49] and are distinctly higher than the experimental data from Ref. 32.

Comparison of the experimental TCSs for the family of methyl-substituted C_nH_{2n} molecules has also been made and similarities and differences have been pointed out and discussed. Based on TCS experimental data for isomers of C_5H_{10} and C_6H_{12} compounds, the isomer effect has also been examined.

ACKNOWLEDGMENTS

This work is part of the MNiSzW Program 2014–2015 and is supported by the Polish Ministry of Science and Higher Education. This work was conducted within the framework of the COST Action CM1301 (CELINA). Numerical computations have been performed at the Academic Computer Center (TASK) in Gdańsk.

[1] *Photon and Electron Interactions with Atoms, Molecules and Ions*, Landolt-Börnstein, Vol. 17, edited by Y. Itikawa (Springer, Berlin, 2000-2003).
[2] L. G. Christophorou and J. K. Olthoff, *Fundamental Electron Interactions with Plasma Processing Gases* (Kluwer/Plenum, NY, 2004).
[3] G. G. Raju, *Gaseous Electronics: Tables, Atoms, and Molecules* (CRC Press, Boca Raton, FL, 2011) and comprehensive references therein.
[4] K. D. Jordan and P. D. Burrow, J. Am. Chem. Soc. **102**, 6882 (1980).
[5] H. H. Brongersma, Ph.D. thesis, Leiden University, 1968.
[6] Cz. Szmytkowski, P. Możejko, and G. Kasperski, J. Phys. B **30**, 4363 (1997); **31**, 3917 (1998); Cz. Szmytkowski and P. Możejko, Vacuum **63**, 549 (2001).
[7] M. Knudsen, Ann. Phys. Lpz. **336**, 205 (1910).
[8] B. Bederson and L. J. Kieffer, Rev. Mod. Phys. **43**, 601 (1971).
[9] J. P. Sullivan, J. Makochekanva, A. Jones, P. Caradonna, D. S. Slaughter, J. Machacek, R. P. McEachran, D. W. Mueller, and S. J. Buckman, J. Phys. B **44**, 035201 (2011).

[10]R. N. Nelson and S. O. Colgate, Phys. Rev. A **8**, 3045 (1973).
[11]P. Możejko, B. Żywicka-Możejko, and Cz. Szmytkowski, Nucl. Instrum. Methods Phys. Res., Sect. B **196**, 245 (2002).
[12]P. Możejko and L. Sanche, Radiat. Environ. Biophys. **42**, 201 (2003); Radiat. Phys. Chem. **73**, 77 (2005).
[13]N. F. Mott and H. S. W. Massey, *The Theory of Atomic Collisions* (Oxford University Press, Oxford, 1965).
[14]K. N. Joshipura and M. Vinodkumar, Z. Phys. D **41**, 133 (1997).
[15]F. Salvat, J. D. Martinez, R. Mayol, and J. Parellada, Phys. Rev. A **36**, 467 (1987).
[16]N. T. Padial and D. W. Norcross, Phys. Rev. A **29**, 1742 (1984).
[17]J. P. Perdew and A. Zunger, Phys. Rev. B **23**, 5048 (1981).
[18]X. Zhang, J. Sun, and Y. Liu, J. Phys. B **25**, 1893 (1992).
[19]Y.-K. Kim and M. E. Rudd, Phys. Rev. A **50**, 3954 (1994); W. Hwang, Y.-K. Kim, and M. E. Rudd, J. Chem. Phys. **104**, 2956 (1996).
[20]M. J. Frisch *et al.*, GAUSSIAN 03, Revision B.03, Gaussian, Inc., Pittsburgh, PA, 2003.
[21]L. S. Cederbaum, J. Phys. B **8**, 290 (1975).
[22]W. von Niessen, J. Schirmer, and L. S. Cederbaum, Comput. Phys. Rep. **1**, 57 (1984).
[23]J. V. Ortiz, J. Chem. Phys. **89**, 6348 (1988).
[24]V. G. Zakrzewski and W. von Niessen, J. Comput. Chem. **14**, 13 (1994).
[25]P. Możejko, E. Ptasińska-Denga, A. Domaracka, and Cz. Szmytkowski, Phys. Rev. A **74**, 012708 (2006).
[26]P. Możejko, A. Domaracka, E. Ptasińska-Denga, and Cz. Szmytkowski, Chem. Phys. Lett. **429**, 378 (2006).
[27]Cz. Szmytkowski, P. Możejko, E. Ptasińska-Denga, and A. Sabisz, Phys. Rev. A **82**, 032701 (2010).
[28]P. Możejko, E. Ptasińska-Denga, Cz. Szmytkowski, and M. Zawadzki, J. Phys. B **45**, 145203 (2012).
[29]P. Możejko, E. Ptasińska-Denga, and Cz. Szmytkowski, Eur. Phys. J. D **66**, 44 (2012).
[30]Cz. Szmytkowski, P. Możejko, M. Zawadzki, and E. Ptasińska-Denga, J. Phys. B **46**, 065203 (2013).
[31]Cz. Szmytkowski, P. Możejko, M. Zawadzki, K. Maciąg, and E. Ptasińska-Denga, Phys. Rev. A **89**, 052702 (2014).
[32]O. Sueoka, C. Makochekanwa, H. Tanino, and M. Kimura, Phys. Rev. A **72**, 042705 (2005).
[33]Cz. Szmytkowski, S. Kwitnewski, and E. Ptasińska-Denga, Phys. Rev. A **68**, 032715 (2003).
[34]Cz. Szmytkowski and S. Kwitnewski, J. Phys. B: At., Mol. Opt. Phys. **35**, 2613 (2002); **35**, 3781 (2002); **36**, 2129 (2003); **36**, 4865 (2003).
[35]This paper.
[36]L. Libit and R. Hoffmann, J. Am. Chem. Soc. **96**, 1370 (1974).
[37]C. R. Bowman and W. D. Miller, J. Chem. Phys. **42**, 681 (1965).
[38]I. C. Walker, A. Stamatovic, and S. F. Wong, J. Chem. Phys. **69**, 5532 (1978).
[39]J. Rutkowsky, H. Drost, and H.-J. Spangenberg, Ann. Phys. **492**, 259 (1980).
[40]R. Panajotovic, M. Kitajima, H. Tanaka, M. Jelisavcic, J. Lower, L. Campbell, M. J. Brunger, and S. J. Buckman, J. Phys. B **36**, 1615 (2003).
[41]M. Allan, C. Winstead, and V. McKoy, Phys. Rev. A **77**, 042715 (2008).
[42]D. F. Dance and I. C. Walker, Proc. R. Soc. A **334**, 259 (1973).
[43]M. Allan and L. Andric, J. Chem. Phys. **105**, 3559 (1996).
[44]C. S. Trevisan, A. E. Orel, and T. N. Rescigno, Phys. Rev. A **68**, 062707 (2003).
[45]Y. Itikawa, Int. Rev. Phys. Chem. **16**, 155 (1997).
[46]K. Floeder, D. Fromme, W. Raith, A. Schwab, and G. Sinapius, J. Phys. B **18**, 3347 (1985).
[47]H. Nishimura and H. Tawara, J. Phys. B **24**, L363 (1991).
[48]C. Makochekanwa, M. Hoshino, H. Kato, O. Sueoka, M. Kimura, and H. Tanaka, Phys. Rev. A **77**, 042717 (2008).
[49]D. Shi, J. Sun, Y. Liu, and Z. Zhu, J. Phys. B **41**, 025205 (2008).
[50]*Handbook of Chemistry and Physics*, 76th ed., edited by D. R. Lide (CRC Press, Boca Raton, 1995-1996).
[51]J. Zhao and R. Zhang, Atmos. Environ. **38**, 2177 (2004).
[52]K. J. Miller, J. Am. Chem. Soc. **112**, 8533 (1990).
[53]A. S. Barbosa and M. H. F. Bettega, J. Chem. Phys. **141**, 244307 (2014).